72th International Astronautical Congress (IAC), Dubai, UAE, 25-29 October 2021.

IAC-21,C1,6,10,x62976

A stable heliocentric disposal strategy for LPO missions, inspired by the natural co-orbital motion of Saturn's moons

A. Pousse[a], E. M. Alessi[a,b]*

[a] *Istituto di Matematica Applicata e Tecnologie Informatiche "E. Magenes", via Alfonso Corti 12, 20133 Milano, Italy* alexandre@mi.imati.cnr.it, elisamaria.alessi@cnr.it
[b] *Istituto di Fisica Applicata "Nello Carrara", Consiglio Nazionale delle Ricerche, Via Madonna del Piano 10, 50019 Sesto Fiorentino (FI), Italy.*
* Corresponding Author

Abstract

In this work, we present a disposal strategy for Sun-Earth LPO missions, based on stable heliocentric graveyard trajectories that do not approach the Earth-Moon system in the long term. Previous studies analyzed the possibility of reentering to the Earth, impacting on the Moon or move to a heliocentric graveyard orbit. The novelty of our work is that we take advantage of the mutual configuration observed in nature between Janus and Epimetheus, two moons of Saturn, to design a heliocentric graveyard strategy that is stable in the long term and does not require additional operations to stay away from the Earth. Rather than lowering the energy of the spacecraft (or increasing the Jacobi constant) to close the zero-velocity curves, the configuration needs an energy increase to reach a trajectory that encompasses L_3, L_4 and L_5. Taking advantage of the theory developed to explain the motion of Janus and Epimetheus, we design horseshoe-shaped orbits, that satisfy the conditions required to be stable under the dominant orbital perturbations. The stability of these disposal orbits is verified considering a $n-$body problem with solar radiation pressure. The transfer required to move from a given L_2 LPO mission to such orbits can be designed exploiting the unstable invariant manifold of the L_2 orbit.

Keywords: Libration Point Orbit mission, Co-orbital motion, End-of-life, Disposal Orbit, Space Situational Awareness

1. Introduction

Libration Point Orbits (LPO) are exploited in the Sun-Earth system since decades to place space observatories for solar and astrophysics purposes. Though not considered protected regions, there exist studies funded by ESA and NASA [1, 2, 3] focusing on the design of end-of-life disposal practices. They are motivated by the increasing awareness of considering orbital regions as unique resources to be preserved for the operational and the planned missions and for the new generations. As far as we know, official guidelines do not exist for Sun-Earth LPO missions, while for Earth-Moon LPO missions a preliminary discussion has started, in view of the forthcoming operations in the cislunar environment [4].

In this work, we propose a disposal strategy for Sun-Earth LPO missions[1], based on stable heliocentric graveyard trajectories that do not approach the Earth-Moon system in the long term. Previous studies analyzed the possibility of reentering to the Earth [1, 2, 5, 6, 7], impacting on the Moon [1, 2, 8] or move to a heliocentric graveyard orbit [1, 2, 3, 9]. As regards to the third option, that is actually the only one implemented so far (see, e.g., [10, 11]), the idea is to move the spacecraft beyond the zero-velocity curves (ZVC), interior to L_1 or exterior to L_2 (depending on the operational orbit), and eventually apply an impulsive maneuver[2] to close the ZVC to prevent the spacecraft from returning to the Earth's neighborhood. In this case, Monte Carlo simulations are usually required to evaluate the risk of an Earth's return in the long term (about 100 years), by considering a full dynamics that accounts for the main orbital perturbations [14]. Another possibility is to take advantage of the natural third-body perturbation due to the Earth to increase continuously the

[1] in what follows, denoted as just LPO missions.

[2] or exploit the solar radiation pressure to the same end [12, 13].

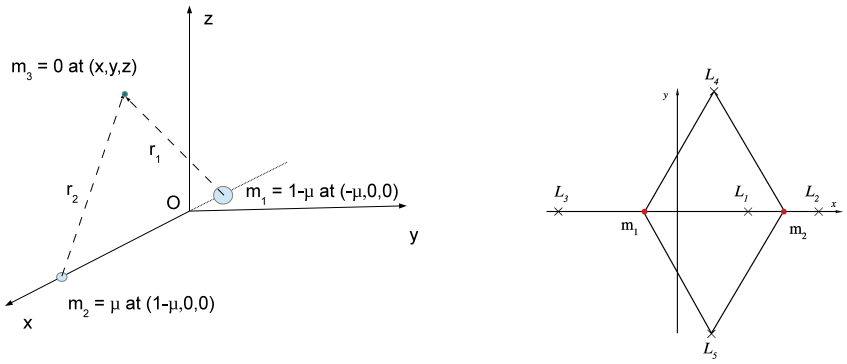

Figure 1: The synodic reference system for the CR3BP and the equilibrium points (right).

Minimum Orbit Intersection Distance [15].

The novelty of this work is that we take advantage of the mutual configuration observed in nature between Janus and Epimetheus [16], two moons that orbit Saturn on horseshoe-shaped trajectories, to design a heliocentric graveyard strategy that is stable in the long term and does not require additional operations to stay away from the Earth. Rather than lowering the energy of the spacecraft (or increasing the Jacobi constant) to close the ZVC, the configuration needs an energy increase to reach a trajectory that encompasses L_3, L_4 and L_5.

The graveyard options are chosen following the theoretical findings in [16] and [17] and tested in a more comprehensive dynamics that accounts for the solar radiation pressure effect and the gravitational attractions of the planets and the Moon.

In the last part of the work, we design the transfers from planar Lyapunov orbits at L_2 to a selected horseshoe orbits, in terms of stability and energy level. The end-of-life transfer is computed by means of the unstable invariant manifold corresponding to the L_2 orbit.

2. The Circular Restricted Three-Body Problem

Libration Point Orbits are designed in the context of the Circular Restricted Three-Body Problem (CR3BP) [18], the model that studies the behavior of a particle with negligible mass moving in the gravitational field of two primaries of masses m_1 and m_2, each one revolving around their common center of mass on circular orbits. In this work, m_1 is the Sun and m_2 the Earth–Moon barycenter. To remove time dependence from the equations of motion, it is usually introduced a synodic reference system $\{O, x, y, z\}$, that rotates around the z-axis with constant angular velocity equal to the mean motion of the primaries. The origin of the reference frame is set at the barycenter of the system and the x-axis as the line joining the primaries, oriented in the direction of the smallest primary. In this way m_1 and m_2 result to be fixed on the $x-$axis.

The units are chosen to set the gravitational constant, the sum of the masses of the primaries, the distance between them and the modulus of the angular velocity of the rotating frame equal to 1. In the Sun–Earth+Moon system, the unit of distance equals 1 AU = 1.49597870691×10^8 km and the dimensionless mass of the Earth+Moon barycenter is $\mu = \frac{m_2}{m_1+m_2} = 3.0404234 \times 10^{-6}$. As such, the most massive body is located at $(-\mu, 0, 0)$, the second one at $(1-\mu, 0, 0)$ (see Fig. 1) and the equations of motion read

$$\begin{aligned} \ddot{x} - 2\dot{y} &= x - \frac{(1-\mu)}{r_1^3}(x+\mu) - \frac{\mu}{r_2^3}(x-1+\mu), \\ \ddot{y} + 2\dot{x} &= y - \frac{(1-\mu)}{r_1^3}y - \frac{\mu}{r_2^3}y, \\ \ddot{z} &= -\frac{(1-\mu)}{r_1^3}z - \frac{\mu}{r_2^3}z, \end{aligned} \tag{1}$$

where $r_1 = [(x+\mu)^2 + y^2 + z^2]^{\frac{1}{2}}$ and $r_2 = [(x-1+\mu)^2 + y^2 + z^2]^{\frac{1}{2}}$ are the distances between the particle and the two primaries. This system of equations admits a first integral – the Jacobi integral – given by

$$(x^2+y^2) + 2\frac{1-\mu}{r_1} + 2\frac{\mu}{r_2} + (1-\mu)\mu - \left(\dot{x}^2 + \dot{y}^2 + \dot{z}^2\right) = \mathcal{C}, \tag{2}$$

where $\mathcal{C}$ is the so called Jacobi constant. In what follows, $(x^2+y^2)+2\frac{1-\mu}{r_1}+2\frac{\mu}{r_2}+(1-\mu)\mu$ will be denoted as $2\Omega(x,y,z)$.

In the synodic reference system, there exist five equilibrium points (see Fig. 1), whose elliptic component defines periodic and quasi-periodic orbits in their neighborhood, namely, the Libration Point Orbits, (see, for instance, [19]). If C_i $(i=1,\ldots,5)$ denotes the value of the Jacobi constant at the L_i equilibrium point, the following holds:

$$\mathcal{C}_1 > \mathcal{C}_2 > \mathcal{C}_3 > \mathcal{C}_4 = \mathcal{C}_5 = 3.$$

In Tab. 1 the values of $\mathcal{C}_1, \mathcal{C}_2, \mathcal{C}_3$ for the Sun-Earth system are given.

$\mathcal{C}_1$	$\mathcal{C}_2$	$\mathcal{C}_3$
3.00090098	3.00089693	3.00000608

Table 1: Values of $\mathcal{C}_1, \mathcal{C}_2, \mathcal{C}_3$ for the Sun-Earth system.

Depending on the value of the Jacobi constant, it is possible to know where the particle can move in the configuration space. According to (2), the regions where the motion is forbidden are characterized by $2\Omega(x,y,z)-\mathcal{C}<0$ and their boundaries are the zero-velocity surfaces (zero-velocity curves in the planar case).

The collinear points L_1, L_2, L_3 are also characterized by one hyperbolic component, and thus stable and unstable invariant manifolds arise from the corresponding point and LPO. By definition, the energy, or Jacobi constant associated with the hyperbolic invariant manifolds stemming from the give equilibrium point is the one given in Tab. 1.

2.1 L_2 Lyapunov orbits

We assume that the operational orbit is a planar Lyapunov orbit at L_2. In Fig. 2, we show some examples. The planar assumption is taken to simplify the analysis, and focus on the role played by the energy level to design the transfer and for the choice of the final disposal orbit (together with the long-term stability, see Sec. 3.). We recall that planar Lyapunov orbits can be computed starting from a linear approximation in the neighborhood of L_2, considering as basic frequency one the center component of the equilibrium point. The whole family is then found by continuation. The family has the same dynamical behavior as the equilibrium point, that is,

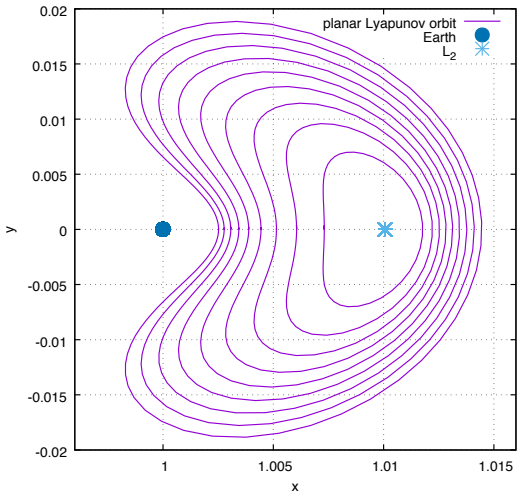

Figure 2: Planar Lyapunov orbits in the neighborhood of L_2. For the orbits shown $\mathcal{C} \in [3.00017641 : 3.00073635]$

there exists a stable invariant and an unstable invariant manifold stemming from the given periodic orbit. We will take advantage to these objects to design the transfer from the operational LPO to the horseshoe disposal orbit.

3. Co-orbital motion and horseshoe-shaped trajectories

3.1 On the Saturn-Janus-Epimetheus system

In the framework of the Three-Body Problem (3BP), the co-orbital motion is associated with trajectories in 1:1 mean-motion resonance. In other words, the two smallest bodies share the same orbital period around a more massive primary.

A major example in the Solar System is given by the Trojan asteroids harboured by Jupiter in the neighbourhood of L_4 and L_5. Another astonishing configuration is given by Janus and Epimetheus, two small moons that orbit Saturn on quasi-coplanar and quasi-circular trajectories whose radii are only 50 km apart, which is less than their respective diameters. Since their orbital period is slightly different, they experience a relatively close approach every 4 years, which leads to a swapping of the orbits: the outer moon becomes the inner one and vice-versa. As Fig. 3 shows, this behavior generates horseshoe-shaped trajectories depicted in an appropriate rotating frame.

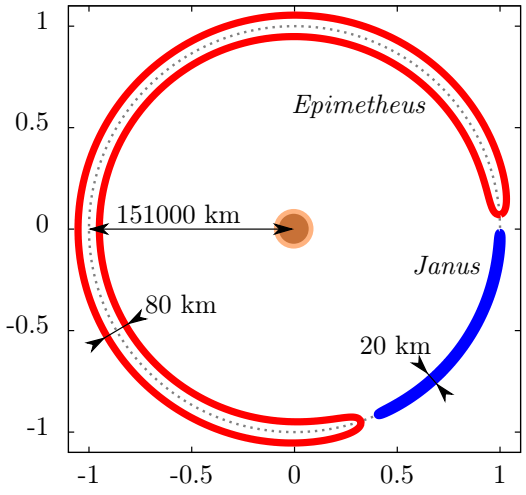

Figure 3: Schematic representation of the Saturn-Janus-Epimetheus trajectories which are depicted in an appropriate rotating frame that rotates with the moons' average mean-motion. They describe a horseshoe shape. It takes about 4 years between each orbital exchange and about 8 years for Janus and Epimetheus to cover all their horseshoe-shaped trajectories (which corresponds to 4000 revolutions around Saturn).

This surprising dynamics was confirmed by Voyager 1's flyby in 1981 [20] and observed over the last decades, especially by the Cassini mission. Moreover, analytical theories [21, 22] as well as numerical investigations [23, 24] provided indications on the long-time stability of the "horseshoe motion".

Recently, a rigorous theorem proves the existence of quasi-periodic horseshoe-shaped trajectories in the 3BP, thanks to KAM theory [16]. It confirms that these heliocentric trajectories, even experiencing close approaches with the planet, can be stable in the long term, and thus, that they can be good candidates for a heliocentric graveyard strategy.

This stability result is based on an integrable approximation obtained by a 1:1-resonant normal form, usually known as averaged problem. In the following and without too much detail, we explain how this theory can be applied to the planar CR3BP for a Sun-Earth system in order to define boundaries on the domain of horseshoe motion. For the complete theory, we refer the reader to [17].

3.2 The domain of horseshoe motion in the averaged problem

The averaged problem in the case of 1:1 mean-motion resonance is a perturbative treatment of the Restricted 3BP which consider μ as a small parameter. In such case, the Hamiltonian function of the planar CR3BP given in the heliocentric reference frame, can be split in two terms: an integrable part which corresponds to the unperturbed Kepler motion of the particle, while the other one models the perturbative terms that depend on μ: the gravitational influence of the Earth, the acceleration of the heliocentric frame, and a term associated with our choice of the Kepler problem. In that framework, the motion of the particle is given by the heliocentric orbital elements (a, e, ω, λ), respectively the semi-major axis, the eccentricity, the argument of periaster and the mean longitude. Likewise, the circular orbit of the planet can be described by the semi-major axis $a' = 1$ AU and the mean longitude λ' with a mean-motion $\dot{\lambda} = 1$. At first order, λ circulates with a mean-motion equal to $\sqrt{a}^{-3}$ while a, e and ω remains fixed. However, in the long term, the perturbative terms of the Hamiltonian will generate slow variations a, e and ω.

The co-orbital motion is a type of solutions located on a particular region of the phase space for which $a \simeq a' = 1$ AU. Moreover, it is characterized by a resonant angle $\theta = \lambda - \lambda'$ which oscillates about some particular values. For instance, a horseshoe-shaped orbit is characterized by θ that features very large oscillations centered on 180°. In this region of the phase space, the timescales are separated: λ' is a "fast" angle, while θ and ω undergoes "slow" variations. A classical way to exploit this feature is to replace the original Hamiltonian by another one for which the fast oscillations have been removed of the perturbative terms. For that purpose, an averaging over the period of revolution of the Earth is performed on the Hamiltonian after the introduction of the resonant angle θ. This process defines the averaged problem in the case of 1:1 mean-motion resonance.

In the circular-planar case, another reduction is possible: the averaged Hamiltonian does not depend on ω and the Poincaré variable $\Gamma = \sqrt{a}(1-\sqrt{1-e^2})$ is a conserved quantity. As a consequence, for a fixed Γ, the averaged Hamiltonian is integrable and phase portraits obtained for various values of Γ allow to understand the global dynamics of the 1:1 mean-motion resonance.

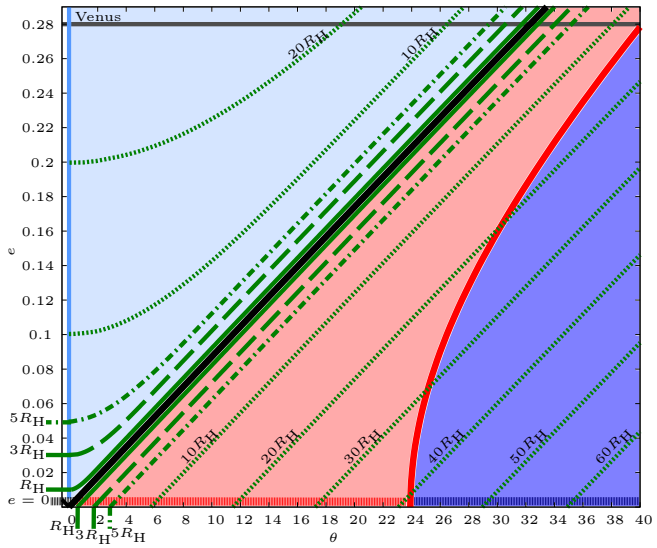

Figure 4: "Map" of the co-orbital motion defined by the section $a = 1$ AU.

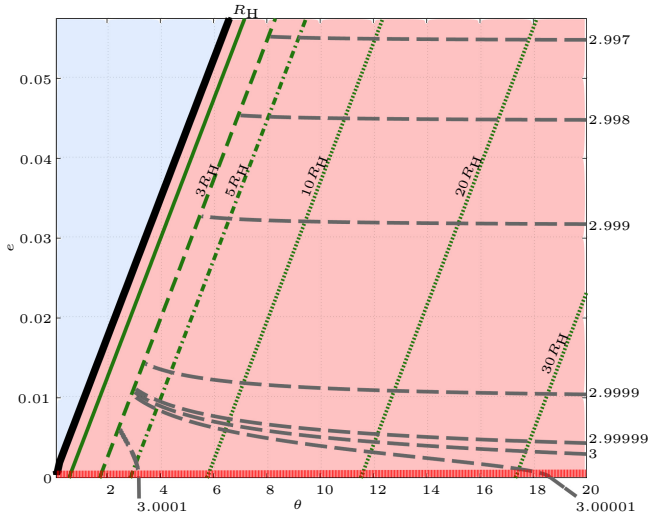

Figure 5: Enlargement in the domain of the horseshoe motion, in the neighborhood of the collision. A dashed grey curve corresponds to the elements (θ, e) for which the Jacobi constant $\mathcal{C}$ is fixed.

Fig. 4 displays the "map" of the co-orbital motion for the Sun-Earth system. It is a synthetic representation of the phase space associated with the section $a = 1$ and for which the boundaries of the horseshoe motion are neatly defined. For instance, the domain of horseshoe motion is bounded by the black thick curve which illustrates the collision with the planet, and by the red thick curve which plots the cross section of the separatrices that originate from L_3 and from the Lyapunov family of L_3. However, since it has been proved that the averaged problem is a reliable approximation of the R3BP as long as the solutions are located outside the Hill's sphere of the Earth (see [17]), (θ, e) must be chosen below the green thick curve, which represents a minimal distance between the Earth and the particle equals to a Hill's radius (denoted $R_H = (\mu/3)^{1/3}$ on Fig. 4 and Fig. 5).

In a more practical way, an initial condition (a, e, ω, λ), such that $a = 1$, $\lambda = \theta + \lambda'$ with (θ, e) that belongs to the red region and $\omega, \lambda' \in \mathbb{T}$ arbitrarily chosen, will provide a quasi-periodic horseshoe-shaped orbit in the averaged problem which approximates, for a finite time, the motion of a particle that starts at the same initial condition in the planar R3BP. More precisely, transitions to another co-orbital motion or escapes from the 1:1 mean-motion resonance can not occur at least during a time $\mathcal{T} = \sqrt{\Delta/R_H}^3$ where Δ corresponds to the minimal distance with respect to the Earth. For instance, it ensures that a trajectory whose initial condition is located in the red region and below the dashed line corresponding to $10R_H$ remains in horseshoe motion for at least 30 years.

A disposal orbit requires long-term stability (centuries) and also to experience relatively close approaches with the Earth in order to be able to construct a transfer with reasonable costs. In this framework, the theoretical result of stability restricts the choice to initial conditions located at a greater distance than 25 Hill's radii. Although the theory cannot ensure it, some horseshoe trajectories can be stable for very long term for closest approaches. To go further, we realize a preliminary investigation of stable horseshoe-shaped trajectories in the CR3BP. Thus, for (θ, e) chosen with a minimal distance Δ smaller than 6 Hill's radii the two following initial conditions can be identified with an important time of stability:

- HS_1: $a = 1$, $e = 0$, $\theta = 3.4925°$, $\omega = -\theta$
- HS_2: $a = 1$, $e = 0.05$, $\theta = 9°$, $\omega = -\theta$

whose respective Jacobi constant are equal to $\mathcal{C} = 3.00009066$ and $\mathcal{C} = 2.99752123$. HS_1 and HS_2 were propagated in the CRTBP for respectively 200 years and 10000 years and Fig. 6 shows that the two solutions correspond to stable horseshoe-shaped trajectories.

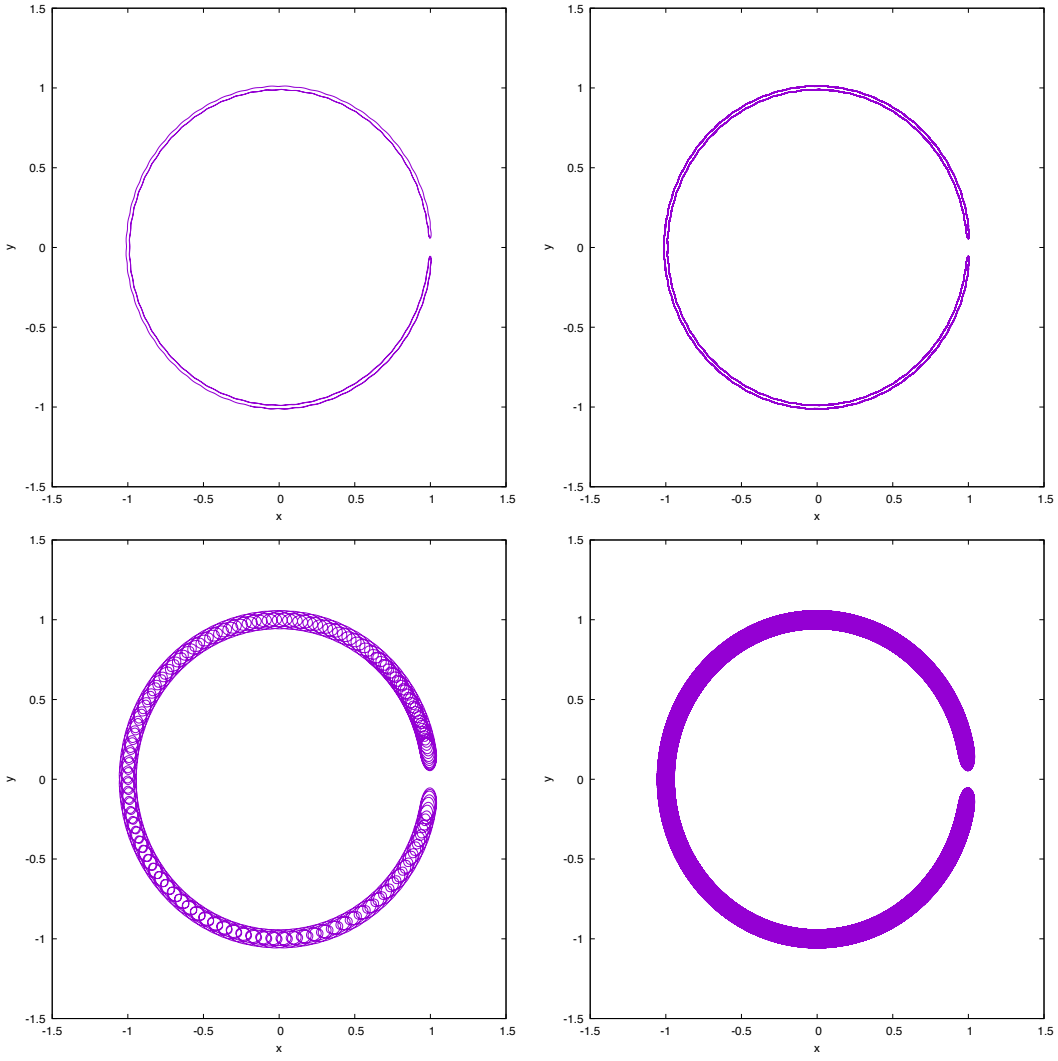

Figure 6: Left: the orbits obtained propagating the CR3BP for 200 years. Right: the orbits obtained propagating the CR3BP for 10000 years Top: Initial condition HS_1. Bottom: Initial condition HS_2.

4. Full dynamics

The final disposal orbit is validated in a full dynamical model, whose equations of motion are written in the geocentric equatorial reference system, denoted as $\{O, \xi, \eta, \zeta\}$, with physical units of distance, time and mass (AU, day and kg). The dynamical effects considered are the main perturbations that might act on LPO and the graveyard orbit [5, 25], that is, the gravitational acceleration due to Sun, Earth, Moon and the planets and the solar radiation pressure. Atmospheric drag and geopotential are not considered because of the distance of the graveyard orbit with respect to the Earth.

The gravitational acceleration (subscript g) exerted on the spacecraft by Sun, Moon and the planet is modeled as

$$\begin{aligned} \ddot{\xi}_g &= -\sum_{p=1}^{11} Gm_p \frac{(x_E - x_p + \xi)}{r_{Ep}^3} - \ddot{x}_E, \\ \ddot{\eta}_g &= -\sum_{p=1}^{11} Gm_p \frac{(y_E - y_p + \eta)}{r_{Ep}^3} - \ddot{y}_E, \\ \ddot{\zeta}_g &= -\sum_{p=1}^{11} Gm_p \frac{(z_E - z_p + \zeta)}{r_{Ep}^3} - \ddot{z}_E, \end{aligned} \tag{3}$$

where

- $(x_p, y_p, z_p, \dot{x}_p, \dot{y}_p, \dot{z}_p)$ is the state vector in the equatorial reference system centered at the Solar System barycenter of the body P of mass m_p and it is evaluated, at a given instant of time, from the JPL ephemeris DE405 [26];
- $(x_E, y_E, z_E, \dot{x}_E, \dot{y}_E, \dot{z}_E)$ is the Earth's state vector in the equatorial reference system centered at the Solar System barycenter, and it is also given by the JPL ephemeris DE405 at each instant of time;
- $r_{Ep} = \sqrt{(x_E - x_p + \xi)^2 + (y_E - y_p + \eta)^2 + (z_E - z_p + \zeta)^2}$.

The effect due to the solar radiation pressure (subscript SRP) follows the so-called cannonball model, and can be seen as the effect due to a residual mass of the Sun, namely,

$$\begin{aligned} \ddot{\xi}_{SRP} &= -C_R \bar{P} a_\odot^2 \frac{A}{m} \frac{(x_E - x_S + \xi)}{r_{ES}^3} \\ \ddot{\eta}_{SRP} &= -C_R \bar{P} a_\odot^2 \frac{A}{m} \frac{(y_E - y_S + \eta)}{r_{ES}^3}, \\ \ddot{\zeta}_{SRP} &= -C_R \bar{P} a_\odot^2 \frac{A}{m} \frac{(z_E - z_S + \zeta)}{r_{ES}^3}, \end{aligned} \tag{4}$$

where C_R is the reflectivity coefficient, $\bar{P} = 4.51 \times 10^{-6}$ N/m^2 is the mean solar radiation pressure at 1 AU, $a_\odot = 1$ AU is the mean distance between the Sun and the Earth, A/m is the area-to-mass ratio and the subscript S denotes the Sun. For the simulations, we assume $C_R A/m = 0.02$ m^2/kg.

4.1 Examples

In Fig. 7, we show two examples of propagation starting from J2000 up to 200 years, assuming the dynamical model just introduced. We have considered the two different initial conditions denoted HS_1 and HS_2, as explained in Sec. 3.. The same figure shows that the distance to the Earth never drops below 2 Hill's radii.

A more systematic study on the long-term behavior of the initial conditions that can be actually exploited for the disposal strategy (see also the considerations in the next section) will be performed in the future.

5. The transfer

In Fig. 8, we show one branch of the unstable manifold associated with two different L_2 Lyapunov orbits (i.e., different values of $\mathcal{C}$), propagated up to 1 year, the corresponding ZVC and two possible disposal horseshoe orbits, namely, one very close to HS_1 and HS_2.

The figure shows clearly how the geometry of the manifold, but also the energy levels corresponding to the LPO and the HS, play a key role in the design of the transfer. In particular, for high values of $\mathcal{C}$ of the LPO and the highest possible value of $\mathcal{C}$ for the HS (top left panel), the HS lies inside the ZVC, and thus the transfer cannot be achieved. As long as the Jacobi constant $\mathcal{C}$ of the LPO decreases, the corresponding ZVC shrinks and an intersection in position can be found (bottom left panel). By considering a more eccentric HS (right panels) an intersection in position can be easily found, but the gap between the two energy levels might be too expensive to fill.

Starting from the definition of the Jacobi constant, Eq. (2), and assuming that the given manifold and HS intersect in position, the minimum impulsive maneuver is a tangent insertion into the HS (see, e.g., [27]), such that

$$\Delta v = \sqrt{v_{man}^2 + v_{HS}^2 - 2 v_{man} v_{HS}}, \tag{5}$$

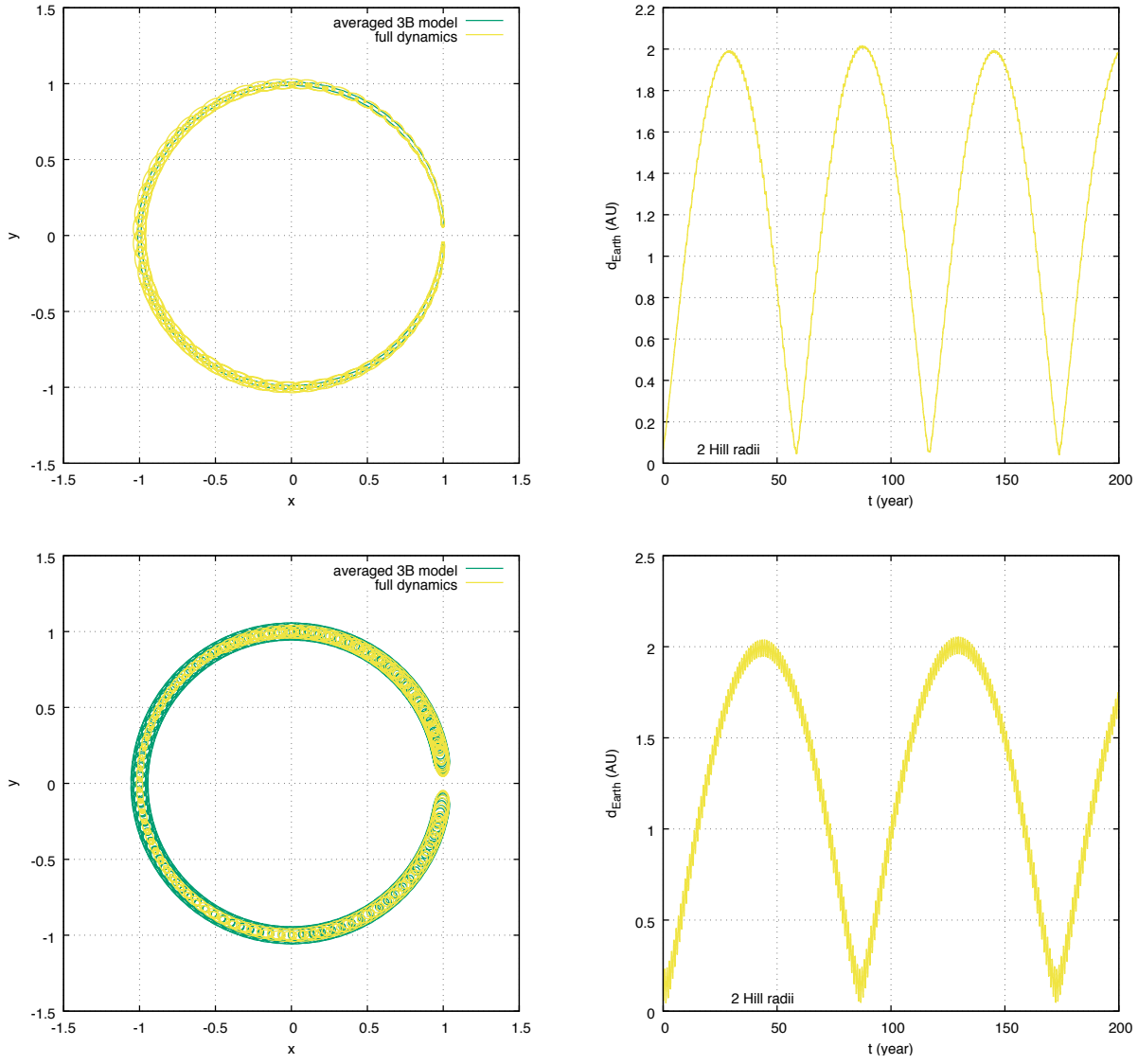

Figure 7: Left: the orbits obtained propagating the CR3BP for 200 years (green) considering as initial condition the one given by the averaged model and the ones obtained propagating the full dynamical model for 200 years (yellow). Right: the distance with respect to the Earth as a function of time, computed with the full dynamical model. Top: Initial condition HS_1. Bottom: Initial condition HS_2.

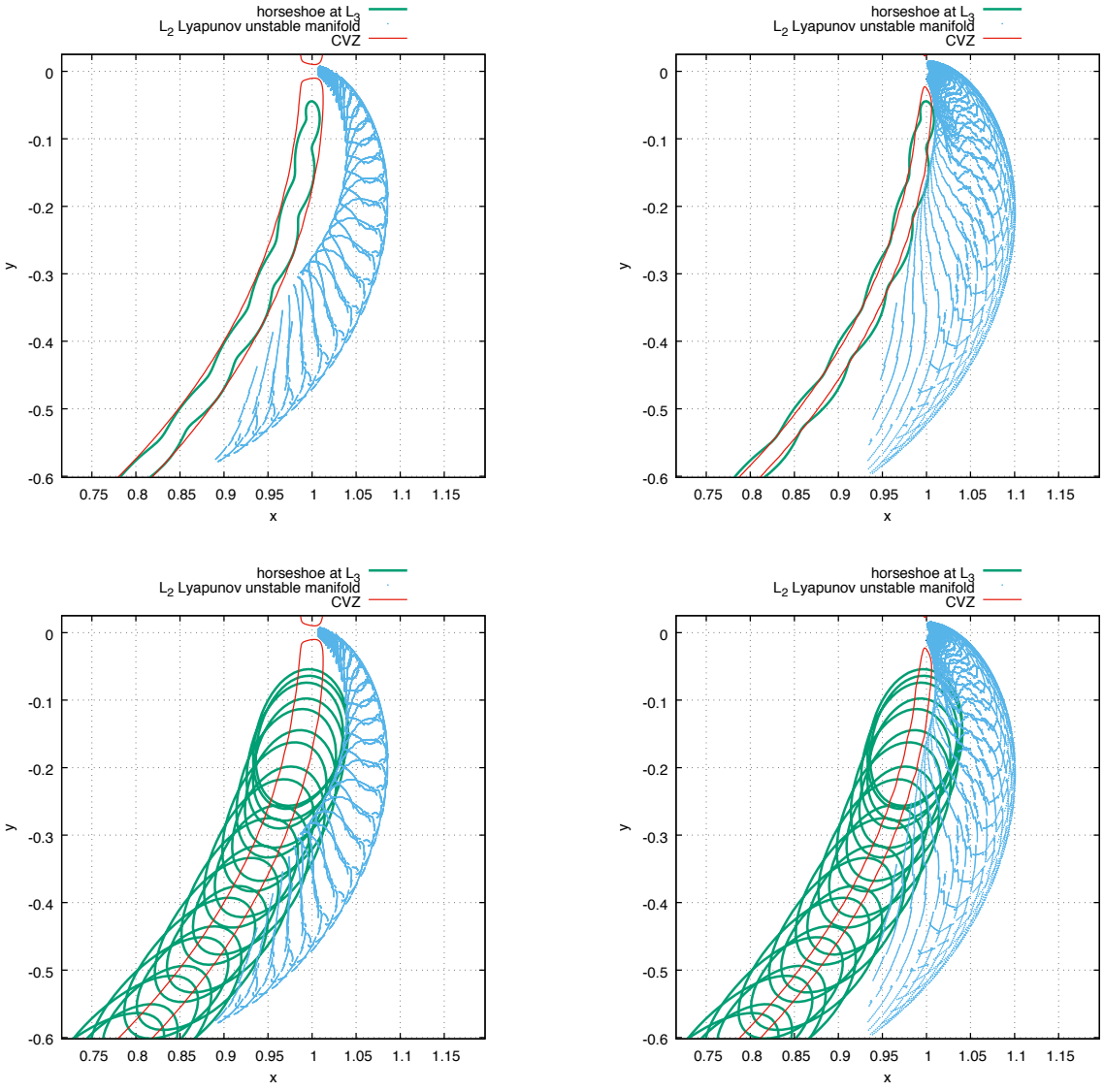

Figure 8: One of the branch of the unstable invariant manifold of a given L_2 Lyapunov orbit (cyan), the ZVC (red) for the corresponding $\mathcal{C}$ and one possible stable disposal horseshoe orbit. Left: $\mathcal{C} = 3.00073635$. Right: $\mathcal{C} = 3.00029812$. Top: Initial condition HS_1. Bottom: Initial condition HS_2.

where $v_{man} = \sqrt{2\Omega(x_{HS}, y_{HS}, z_{HS}) - \mathcal{C}_{man}}$ and $v_{HS} = \sqrt{2\Omega(x_{HS}, y_{HS}, z_{HS}) - \mathcal{C}_{HS}}$. In Fig. 9, we show the minimum cost obtained to move to the HS orbit with the highest possible value of Jacobi constant, $\mathcal{C} = 3.00010012$. Following the study [1] and the actual disposal plan implemented by Herschel [10], we can assume that there might exist LPO missions that can spend up to 200 m/s for the disposal phase. Assuming this value as the maximum available $\Delta v-$budget, it means that the operational LPO must have a Jacobi constant lower than $\mathcal{C} \cong 3.0004$. For a real three-dimensional mission, a possible way to meet this requirement and satisfy also communication constraints (i.e., not considering an orbit with a too large out-of-plane $z-$amplitude) is to consider a Lissajous orbit, to play with the in-plane and the out-of-plane amplitudes.
In the same figure, it is possible to notice a cusp associated with $\mathcal{C} \approx 3.0001$. In this case, in Eq. (5) the contribution given by $v_{man}^2 + v_{HS}^2$ and the one corresponding to $2v_{man}v_{HS}$ cancel out. The value of $\mathcal{C}$ where the cusp may arise depends on the value of $\mathcal{C}$ of the HS target orbit.

Other options of transfer can consider to split the maneuver in two stages, when the manifold and the HS do no intersect in position, or the usage of low-thrust propulsion as done in [28]. Future work includes a systematic study on the possible transfers that can be designed. The authors in [28] already paved the way in this direction, but a further detailed investigation is needed.

In Fig. 10, we show an example of transfer that cost about 140 m/s from a L_2 Lyapunov orbit with $\mathcal{C} = 3.00025095$ to the HS orbit with the highest possible value of Jacobi constant, $\mathcal{C} = 3.00010012$.

6. Conclusions

This work presents a novel disposal option for Libration Point Orbits missions in the Sun-Earth system, inspired by the natural real motion of two moons of Saturn. Beyond the concrete advantages offered by the horseshoe orbits, the study also aims at showing how a robust analytical understanding of the dynamics is key to provide an aware solution of practical problems, in terms of numerical cost and global view. From the one hand, the perturbative treatment of the CR3BP considered shows where the solutions of interest can be found, without implementing expensive numerical simulations. On the other hand, as also already stated by various investigations in the field, the end-of-life phase of a mission must be planned in advance and the mission design must take it into account. In the specific case considered here, this means to choose the size (and thus the energy) of the operational LPO also depending on the disposal strategy. Finally, celestial mechanics lays the foundation of both space engineering and planetary sciences and the two disciplines must learn more and more to interact and help each other.

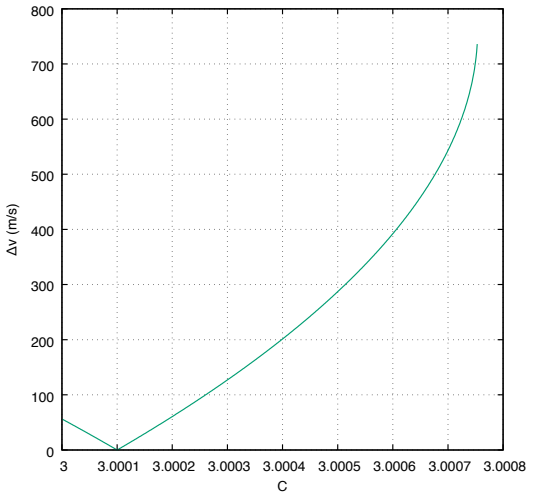

Figure 9: Estimate of the cost required to move from a LPO characterized by $\mathcal{C}$ to the horseshoe orbit with the highest possible value of Jacobi constant, $\mathcal{C} = 3.00010012$.

Acknowledgements

E. M. Alessi is grateful to J. P. Sánchez Cuartielles, E. Fantino and A. Farrés for their valuable suggestions and constructive discussions.
This work is part of the project entitled “co-orbital motion and three-body regimes in the solar system”, funded by Fondazione Cariplo through the program “Promozione dell’attrattività e competitività dei ricercatori su strumenti dell’European Research Council – Sottomisura rafforzamento".

References

[1] Colombo C, Alessi EM, van der Weg W, Soldini S, Letizia F, Vetrisano M, et al. End-of-life disposal concepts for Libration Point Orbit and Highly Elliptical Orbit missions.

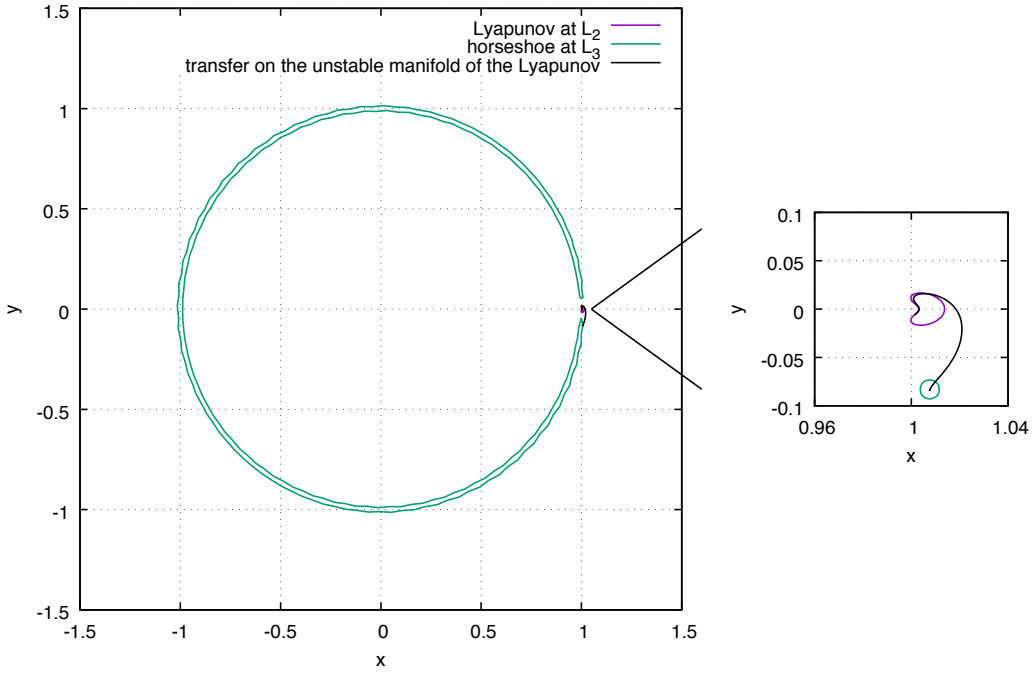

Figure 10: Example of transfer achievable completely on the unstable invariant manifold of the given LPO.

Acta Astronaut 2015; 110: 298-312. doi: 10.1016/j.actaastro.2014.11.002

[2] Armellin R, Rasotto M, Di Lizia P, Renk F. End-of-life disposal of libration point orbit missions: The case of Gaia. Adv Space Res 2015; 56(3):461-78. doi:10.1016/j.asr.2015.03.014.

[3] Petersen JD, Brown JM. End of life disposal for three libration point missions through manipulation of the Jacobi constant and zero velocity curves. In: Advances in the Astronautical Sciences Astrodynamics 2015; 156: AAS 15-618.

[4] Pollock GE, Vedda JA. Cislunar stewardship: planning for sustainability and international cooperation. The Aerospace Corporation 2020. https://aerospace.org/paper/cislunar-stewardship-planning-sustainability-and-international-cooperation

[5] Alessi EM. The reentry to Earth as a valuable option at the end-of-life of Libration Point Orbit missions. Adv Space Res 2015; 55(12):2914-30. doi:10.1016/j.asr.2015.03.012.

[6] Alessi EM, Tommei G, Holbrough I, Beck J. Dynamical uncertainty and demisability occurrence for the atmospheric re-entry of SOHO. Adv Space Res 2018; 62(11):3033-47. doi:10.1016/j.asr.2018.08.019.

[7] Tommei G, Alessi EM. Studying a Direct Re-Entry from a Sun-Earth Libration Point Orbit: Can Ground Uncertainty be Kept Under Control? In: Proc. First International Orbital Debris Conference 2019, Sugar Land, Texas. LPI Contribution No. 2109. id. 6073

[8] van der Weg W, Vasile M. Sun-Earth L_1 and L_2 to Moon transfers exploiting natural dynamics. Celest Mech Dyn Astr 2014; 120: 287-308. doi: 10.1007/s10569-014-9581-4.

[9] Olikara ZP, Gómez G, Masdemont JJ. Dynamic Mechanisms for Spacecraft Disposal from Sun Earth Libration Points. J Guid Control Dyn 2015; 38(10): 1976-89. doi:10.2514/1.G000581.

[10] Keck F. Herschel Post Helium Tests And Spacecraft Disposal Plan. ESA PT-HMOC-OPS-PL-6227-OPS-OAH Document 2013.

[11] http://sci.esa.int/herschel/52797-herschelstatus-report-05-2013

[12] Soldini S, Colombo C, Walker S. The end-of-life disposal of satellites in libration-point orbits using solar radiation pressure. Adv Space Res 2016; 57(8): 1664-79. doi: 10.1016/j.asr.2015.06.033.

[13] Soldini S, Colombo C, Walker S. Solar Radiation Pressure Hamiltonian Feedback Control for Unstable Libration-Point Orbits. J Guid Control Dyn 2017; 40(6): 1374-89. doi: 10.2514/1.G002090.

[14] Colombo C, Letizia F, Soldini S, Renk F. Disposal of Libration Point Orbits on a Heliocentric Graveyard Orbit: the Gaia mission. In: Proc. 25th International Symposium on Space Flight Dynamics 2015, Munich, Germany.

[15] Alessi EM, Sánchez Cuartielles JP. MOID-Increasing Disposal Strategies for LPO Missions. In: Proc. 65th International Astronautical Congress 2014, Toronto, Canada, paper 14.C1.8.12, 2014.

[16] Niederman L, Pousse A, Robutel P. On the Co-orbital Motion in the Three-Body Problem: Existence of Quasi-periodic Horseshoe-Shaped Orbits. Commun Math Phys 2020; 377: 551-612. doi: 10.1007/s00220-020-03690-8

[17] Pousse A, Alessi EM. Revisiting the averaged problem in the case of mean-motion resonances of the restricted three-body problem. Global rigorous treatment and application to the co-orbital motion. arXiv preprint. arXiv:2106.14810, 2021.

[18] Szebehely V. Theory of orbits. New York: Academic Press; 1967.

[19] Gómez G, Mondelo, JM. The dynamics around the collinear equilibrium points of the RTBP. Physica D 2001; 157(4):283-321. doi:10.1016/S0167-2789(01)00312-8.

[20] Aksnes, K. The tiny satellites of Jupiter and Saturn and their interactions with the rings. In Szebehely, V. G., editor, *NATO (ASI) Series C*, volume 154 of NATO (ASI) Series C, pages 3–16, 1985.

[21] Dermott SF, Murray CD. The dynamics of tadpole and horseshoe orbits II. The coorbital satellites of Saturn. Icarus 1981; 48:12–22. doi:10.1016/0019-1035(81)90148-2

[22] Yoder, CF, Colombo G, Synnott, SP, Yoder KA. Theory of motion of Saturn's coorbiting satellites. Icarus 1983; 53:431–443. doi:10.1016/0019-1035(83)90207-5

[23] Llibre, J, Ollé M. The motion of Saturn coorbital satellites in the restricted three-body problem. Astronomy and Astrophysics 2001; 378:1087–1099. doi:10.1051/0004-6361:20011274.

[24] Barrabés E, Ollé M. Invariant manifolds of L3 and horseshoe motion in the restricted three-body problem. Nonlinearity 2006; 19:2065–2089. doi: 10.1088/0951-7715/19/9/004.

[25] Milani A, Nobili A, Farinella P. Non-gravitational perturbations and satellite geodesy. Bristol and Boston: Adam Hilger Ltd., 1987.

[26] Standish EM. JPL Planetary and Lunar Ephemerides, DE405/LE405. Jet Propulsion Laboratory Memorandum IOM 312.F-98-048, Pasadena, 1998.

[27] Alessi EM, Gómez G, Masdemont JJ. Two-maneuvers transfer between LEOs and Lissajous orbits in the Earth-Moon system. Adv Space Res 2010; 45: 1276-1291. doi: 10.1016/j.asr.2009.12.010.

[28] Tantardini M, Fantino E, Ren Y, Pergola P, Gómez G, Masdemont JJ. Spacecraft trajectories to the L_3 point of the Sun-Earth three-bdoy problem. Celest Mech Dyn Astr 2010; 108: 215-232. doi: 10.1007/s10569-010-9299-x.